Investigation of Imprint in FE-HfO_2 and its Recovery

Y. Higashi, B. Kaczer, A. S. Verhulst, B. J. O'Sullivan, N. Ronchi, S. R. C. McMitchell, K. Banerjee, L. Di Piazza, M. Suzuki, D. Linten, and J. Van Houdt

***Abstract*— Ferroelectric (FE)-HfO_2 based FETs (FEFETs) are one of the most promising candidates for emerging memories. However, the FE material suffers from a unique reliability phenomenon known as imprint: the coercive voltage shifts during data retention, which has been regarded as a major issue for memory operation, while the mechanism causing it is still under research. In this paper, imprint and its recovery in FE-HfO_2 are investigated in detail by comprehensive electrical measurements to reveal its underlying mechanism including the cause of asymmetric coercive voltage shifts. The recovery measurements clarify that domain switching is indispensable for the recovery from imprint. The sub-loop imprint effect shows that imprint and its recovery must be independent for each domain. In addition, switching time measurements and corresponding fitting results with the nucleation-limited-switching (NLS) model strongly indicate that imprint is caused by domain-seeds-pinning. Based on these results, we conclude that charge trapping and de-trapping affecting activation barriers for domain switching, accompanied by domain switching is responsible for imprint and its recovery.**

***Index Terms*— Ferroelectric (FE), hafnium oxide, imprint, recovery, charge trapping, NLS, reliability**

I. Introduction

The FE-HfO_2 based FET (FEFET) is a promising candidate for emerging memories thanks to its numerous advantages over standard non-volatile memory devices, such as higher speed, lower operating voltage, better endurance, and simpler gate stack structure [1] [2]. However, ferroelectric materials are subject to a unique phenomenon: imprint. In this paper, imprint is defined as the coercive voltage (V_c) shift during the data retention. The imprint effect has been regarded as a major issue for memory operation in FEFET. Imprint leads, for example, to a higher operation voltage, resulting in high stress followed by poor endurance and poor data retention [3]. Therefore, understanding the physical origin and mechanism of imprint is important to improve FEFET memory performance.

So far, multiple imprint models have been proposed [4] - [13]. They can be categorized as "domain-pinning" [4] - [9] or "non-domain-pinning" models, such as the stress model [10] and the graded layer model [10] [11]. The imprint is also linked to the FE switching kinetics. Two typical switching kinetics models for ferroelectric films exist. One is the Kolmogorov-Avrami-Ishibashi (KAI) model [14] - [16], and the other is the nucleation-limited-switching (NLS) model [17] [18]. The KAI model assumes that the switching time is dominated by the domain wall expansion. On the other hand, the NLS model assumes that the switching time is dominated by the domain nucleation. The domain-pinning model can be further classified as either a "domain-wall-pinning" [4] [10] or a "domain-seed-pinning" [8], in relation to the kinetics.

The root causes of the domain-pinning are still under research. Although charge injection models for imprint of FE-HfO_2 were recently proposed [8] [9], comprehensive investigations are still required to explain the whole phenomenon of imprint, such as the asymmetric V_c shift [3] and the recovery from imprint [19] [20].

In this paper, comprehensive electrical measurements are presented to clarify the mechanism of imprint and its recovery in FE-HfO_2. The recovery behavior of imprint is investigated, showing the domain-pinning behavior. Then, the domain-seeds-pinning model is investigated by "sub-loop imprint" and switching time measurements. Finally, a charge trapping model is discussed to describe the measurements results.

II. Device and Measurement

The devices used in this work were Al-doped HfO_2 capacitors with a size of 100 μm×100 μm for all measurements except for the switching time measurements. For the switching time measurements, capacitors with a size of 50 μm×50 μm were used in order to lower the RC delay effects (we confirmed that the RC delay did not affect the results in the presented time range > 1 μs by using larger size of capacitors of 100 μm×100 μm). The gate stack structure was Poly-Si/FE-HfO_2 (8 nm)/Si substrate. In transmission electron microscopy (TEM) images, an interfacial layer (IL) was not clearly observed [3], however, for TCAD simulation, we assumed the structure to have a thin oxide IL between HfO_2 and Si substrate, namely Poly-Si/HfO_2(8 nm) /SiO_2(0.5 nm)/Si substrate. The Si substrate and Poly-Si gate were highly p-type and n-type doped, respectively. The FE-HfO_2 was deposited by atomic layer deposition (ALD) with Al as dopant. Post-deposition annealing for 1 min at 850 °C in N_2 ambient was performed to crystallize the FE-HfO_2. Polarization-Voltage (P-V) measurements were carried out using a Keithley 4200 tool with fast pulse measurement capability. The $V_{c\pm}$ was defined as the voltage corresponding to the ± current peak in the

Y. Higashi and M. Suzuki are with the Kioxia corporation assigned at imec (e-mail: yusuke.higashi@kioxia.com).

B. Kaczer, A. S. Verhulst, B. J. O'Sullivan, N. Ronchi, S. R. C. McMitchell, K. Banerjee, L. Di Piazza, and D. Linten are with the imec, Kapeldreef 7, B-3001 Leuven, Belgium.

J. Van Houdt is with the imec, Kapeldreef 75, B-3001 Leuven, Belgium and also with ESAT Department, KU Leuven, Leuven, Belgium.

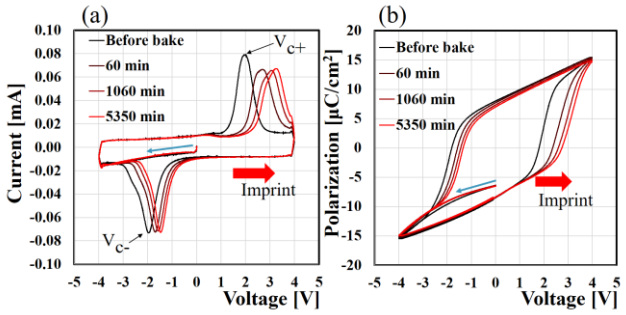

Fig. 1. Al:HfO_2 FE capacitor (a) I-V curves and (b) the corresponding P-V curves measured with a triangular pulse train with segment amplitudes of 0 V, -4V, +4 V, -4 V and 0 V before and after baking at 85ºC. The capacitor was set to the "negative" state before baking [20]. The vertical offsets at the starting points are caused by polarization loss in the time between the end of the cycling and the start of the P-V measurement. The 1st triangular pulse was applied to suppress this polarization loss effect.

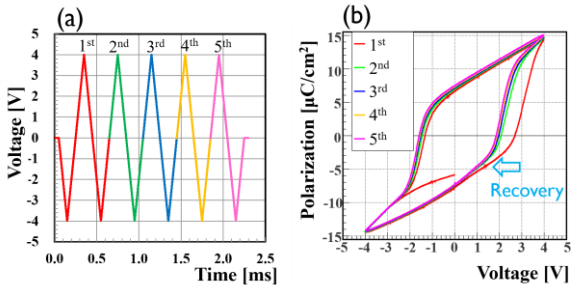

Fig. 2. (a) Waveform of a 5-cycle triangular pulse train applied after baking at the "negative" state at 125 ºC for 90 min and (b) the measured P-V curves. V_c shifts towards negative values after the pulse train [19].

I-V curves (cf. Fig. 1). A triangular pulse with rise time of 100 μs was applied to obtain the P-V hysteresis loop at room temperature (RT). The same triangular pulse, repeated 100 times, was used to induce the wake-up effect on all samples. After that, the samples were baked at different temperatures to induce the imprint effect and re-measured.

III. Results and Discussion

We now show the results to clarify the mechanism of imprint.

1. Recovery from Imprint

Figs. 1(a) and (b) show an example of I-V curves and P-V curves measured before and after baking the capacitor at 85 ˚C. The V_c shift, resulting from imprint, depends on the polarization state before baking. The V_c of samples baked while in the "negative" state shifts in the positive direction. Asymmetric Vc shifts were observed. Namely, the shift in Vc+ was larger than that of Vc- (Fig. 1). Additionally, the V_c of samples baked while in the "positive" state shifts in the negative direction and, similarly to the "negative" state, it was also observed that the shift in V_{c-} was larger than that of V_{c+} (cf. Fig. 6).

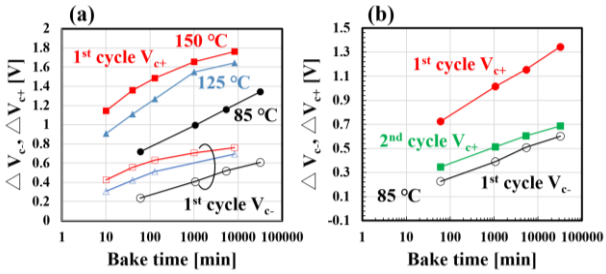

Fig. 3. Median value of (a) 1st cycles V_{c+} (closed symbols) and V_{c-} (open symbols) shift of 18 samples as a function of bake time at 85 ºC, 125 ºC and 150 ºC, and (b) 1st cycles $\Delta V_{c\pm}$ and 2nd cycle ΔV_{c+} as a function of bake time at 85 ºC [19].

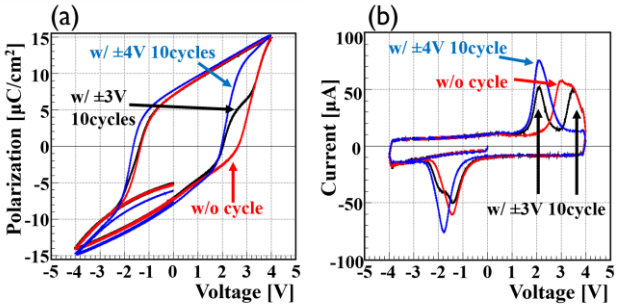

Fig. 4. (a) P-V curves with a triangular pulse train with segment amplitudes of 0 V, -4 V, +4 V, -4V and 0 V and (b) switching current after baking at the "negative" sate with and without a 10-cycle triangular pulse train with amplitudes of ±4 V and ±3 V. Imprint was partially recovered when a ±3 V pulse was applied [19].

To investigate the mechanism of pinning and unpinning domains, recovery from imprint was attempted through electrical measurements. After baking at 125 ºC for 90 min, a 5-cycle triangular pulse train with amplitudes of ±4 V was applied at RT to estimate the recovery from imprint (Fig. 2(a)). As shown in Fig. 2(b), recovery from imprint was successful by applying additional cycles, even at RT. The recovery of V_{c+} from the 1st cycle to the 2nd cycle was the largest.

Next, to investigate the relationship between the asymmetric V_c shifts and the imprint recovery, ΔV_{c+} and ΔV_{c-} (the differences between $V_{c\pm}$ after and before the imprint test), were extracted as a function of bake time at different temperatures (Fig. 3(a)). This was also done before (1st cycle) and after (2nd cycle) recovery (Fig. 3(b)). As already observed in Fig. 1, ΔV_{c+} is larger than ΔV_{c-} for the 1st cycle and the slope of ΔV_{c+} is also larger than that of ΔV_{c-} (Fig. 3(a)). However, after applying an additional cycle, the slope of ΔV_{c+} of the 2nd cycle becomes similar to that of ΔV_{c-} of the 1st cycle (Fig. 3(b)). This result indicates that ΔV_{c+} and ΔV_{c-} follow the same mechanism once domains are switched or, in other words, once domains are switched, the asymmetric V_c shifts disappear and there is the recovery from imprint. We will discuss the root cause of this asymmetry in detail in Section III.3.

To reveal the relationship between switching and imprint recovery, a partial recovery measurement was carried out. After baking at the "negative" state at 150 ºC for 1 hr, a 10-cycle

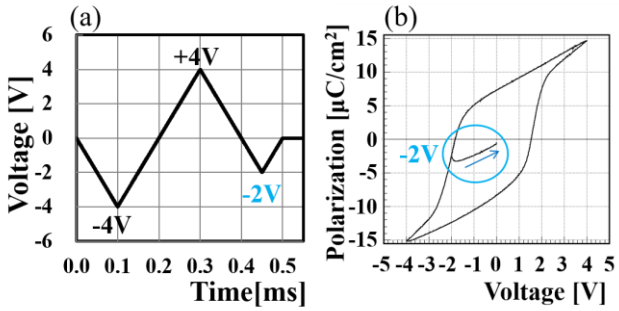

Fig. 5. (a) Waveform of the sub-loop pulse and (b) corresponding P-V loop [19].

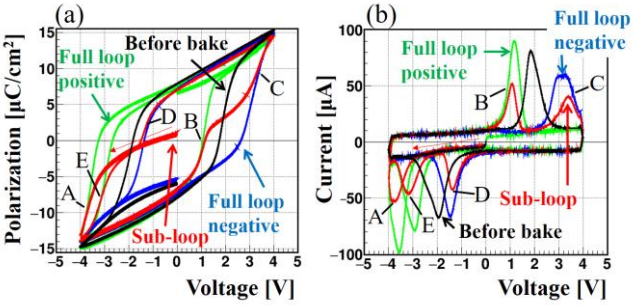

Fig. 6. (a) P-V curves and (b) switching current measured before and after baking for 90 min at 125 ºC with "sub-loop" (see Fig. 5), "full-loop positive" and "full-loop negative" [19].

triangular pulse train with amplitudes of ±4 V or ±3 V were applied to the samples. Imprint was *partially* recovered with the ±3 V pulses, while it was *fully* recovered with the ±4 V pulses, as documented in Figs. 4(a) and (b). These figures show the P-V curves, and the corresponding switching current respectively, and demonstrate the switching voltage distribution of domains. As shown in Fig. 4(a), the P-V curve of the sample subjected to the ±3 V pulses corresponds with that of the sample subjected to the ±4 V pulses up to around +2 V. Moreover, in the region of > +3 V, the P-V corresponds with that of the sample without any pulse (w/o cycle). These results represent the partial recovery phenomenon with ±3 V pulses. As shown in Fig. 4(b), the switching current of the partially-recovered sample with ±3 V pulse has 2 peaks. One peak corresponds to one of the fully-recovered sample, i.e. after application of ±4 V pulses, and the other corresponds to the sample without any recovery pulse (w/o cycle). These results mean that some fraction of domains, switching at voltages less than +3V, are recovered with ±3V pulses, while the rest of the domains, switching at voltages larger than +3V, cannot be recovered at all by ±3V pulses. Namely, imprint can be recovered only because of the switched domains. In other words, if the domains have not switched, the imprint of each domain cannot be recovered even though a high external electric field is applied. These results demonstrate that *the switching of domains is indispensable for imprint recovery of each domain*.

These recovery behaviors are difficult to explain by "non-pinning" model, such as the graded layer model alone [10] [11]. In other words, these results strongly suggest that imprint is caused by domain-pinning. The details are discussed in Section III-3.

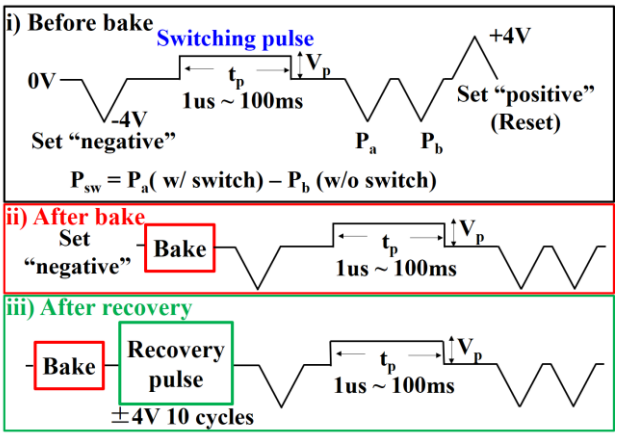

Fig. 7. Measurement sequence of polarization switching time for i) before "bake", ii) after "bake" at 150 ºC for 1hr, and iii) after application of recovery pulse. For cases ii) and iii), a triangular pulse was applied before application of a rectangular pulse to suppress polarization loss effect, and each dataset was measured with different samples.

2. DOMAIN SEEDS PINNING BEHAVIORS

To investigate in detail the pinning behavior mentioned above, a sub-loop pulse was applied to the sample before baking. The measurement sequence was as follows: after wake-up, a triangular pulse train with segment amplitudes of -4 V, +4 V and -2 V was applied, as shown in Fig. 5(a). An example P-V loop before baking is presented in Fig. 5(b). After the sub-loop pulse, the FE-HfO_2 layer simultaneously has both up-state domains and down-state domains. Then, after baking at 125 ˚C for 90 min, a triangular pulse train with amplitude of ±4 V was applied to obtain the P-V hysteresis loop at RT. Additionally, full-loop tests were carried out on different samples for comparison. For these, a triangular pulse train with segment amplitudes of, -4 V, +4 V and -4 V ("full-loop negative"), or +4 V, -4 V and +4 V ("full-loop positive"), were applied before baking.

Fig. 6(a) shows P-V curves "Before bake", "After bake with full-loop positive", "After bake with full-loop negative", and "After bake with sub-loop". After baking, the sub-loop sample exhibited both positive and negative direction shifts from "Before bake", see Figs. 6(a) and (b). Similar splitting behavior was reported in the papers [8][9] [21][22]. In addition, the P-V curve of the sub-loop sample matches that of the sample of "full-loop positive" starting around -3.5 V (point A in Fig. 6(a)). Then it starts to shift to the P-V curve of the sample of "full loop negative" at around the polarization of 0 μC/cm^2 (point B in Fig. 6(a)), and matches it at around +3.5 V (point C in Fig. 6(a)). Then, at the subsequent reverse sweep, it starts to shift again to the 2nd cycle P-V curve of the sample of "full loop positive" at around the polarization of 0 μC/cm^2 (point D in Fig. 6(a)))), and matches it at around -3 V (point E in Fig. 6(a)). Remarkably, the 2nd cycle P-V curve of the sample of "full loop positive" showed the imprint recovery, and the 2nd cycle P-V curve of the sub-loop sample matches it. In addition, the peak voltages of the switching current correspond with those of "full-loops positive and negative", as shown in Fig. 6(b). These results indicate that the down-state domains are not affected by the switching of up-state domains, and vice versa. In

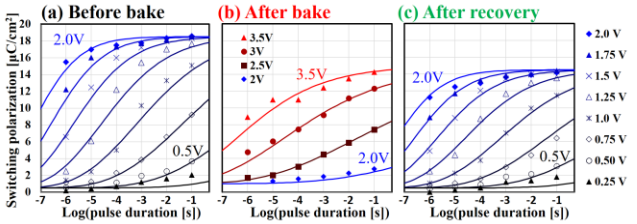

Fig. 8. Switching polarization (P_{sw}) as a function of pulse duration (t_p) at several voltages (V_p) for (a) before bake, (b)

	Before bake	After bake	After recovery
P_0	9 μC/cm²	7 μC/cm²	7 μC/cm²
μ	3.9 MV/cm	4.3 MV/cm	3.9 MV/cm
σ	1.1 MV/cm	1.2 MV/cm	1.1 MV/cm
ΔV	-1.5 V	0 V	-1.5 V

Table I. Extracted NLS parameters of P_0, μ, σ and ΔV.

other words, *the imprint and its recovery of each domain must be independent of other domains*. In addition, these results also show that the imprint of each domain is not affected by the amplitude of a triangular pulse before baking. These results are discussed in detail in Section III-3.

To investigate the imprint behavior in more detail, polarization switching measurements have been carried out. As shown in Fig. 7, after the samples have been set to the "negative" state with a -4 V pulse, rectangular pulses with varying amplitude (V_p) and duration (t_p) have been applied to switch the FE film. Afterwards, two triangular pulses with amplitudes of -4 V are applied to measure polarization, P_a with switching components and P_b without switching components (see Fig. 7). Switching polarization (P_{sw}) is calculated as $P_a - P_b$ in order to subtract leakage components. In addition to the conventional switching time measurement [17] [18], the effect of imprint on switching kinetics was examined by inserting 1 hr "bake" at 150 °C before applying the switching pulses. Moreover, imprint recovery was performed by a 10-cycle triangular pulse train with amplitudes of ±4 V after baking and before the switching pulses.

As shown in Fig. 8(a), the polarization switching time exhibits log-like behavior. As mentioned in the introduction, two typical switching kinetics models for ferroelectric films exist, the KAI model [14] [16] and the NLS model [17] [18]. The KAI model assumes that the switching time is dominated by the domain wall expansion. However, it cannot explain the logarithmic slope of the switching time. On the other hand, the NLS model assumes that the switching time is dominated by the domain nucleation, which can explain the logarithmic slope with the assumption of exponential distribution of switching wait times of individual domain seeds. In addition, there are 2 formulations of NLS. One is using τ_{max} and τ_{min} to characterize the data at various voltages [17] [18] [20]. The other is using the Merz law [23]-[26]. In this paper, the data points were fitted by the latter by using a log-normal distribution for the probability density function (PDF) of the activation field for domain switching, E_a:

$$P(t_p,\ V_p) = 2P_0 \int_0^{\infty} \left[1 - e^{-\left(\frac{t_p}{\tau}\right)^n}\right] f(E_a) dE_a \quad (1)$$

$$\tau(V_{p,}\ E_a) = \tau_0 \exp\left\{k\left(\frac{E_a t_{FE}}{(V_p - \Delta V)}\right)^{\alpha}\right\} \quad (2)$$

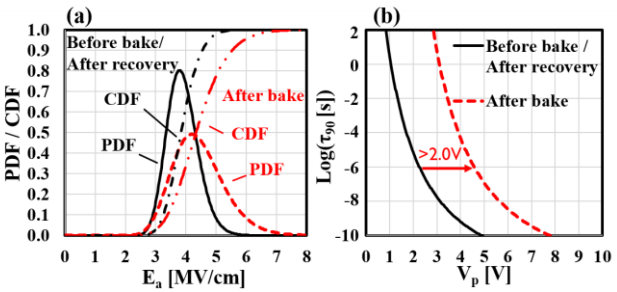

Fig. 9. (a) PDF and CDF as a function of E_a described by (3) and (b) switching time constants with the E_a corresponding to the CDF of 0.9, τ_{90}, as a function of V_p extracted by (2) before and after baking for 1hr at 150°C.

$$f(E_a) = \frac{1}{E_a \ln(\sigma)\sqrt{2\pi}} \exp\left(-\frac{(ln(E_a) - \ln(\mu))^2}{2(\ln(\sigma))^2}\right), \quad (3)$$

where $P(t_p, V_p)$, V_p, t_p, $\tau(V_p, E_a)$, t_{FE}, $f(E_a)$ τ_0, P_0, μ and σ represent switching polarization, pulse amplitude, pulse duration, polarization switching time constant, thickness of FE-HfO_2, PDF of E_a, intrinsic switching time, polarization amplitude, median of $f(E_a)$, and shape parameter of $f(E_a)$, respectively. Furthermore, n, k and α are fitting parameters, respectively. As a side note, if the parameter n was set to n >2, it does not affect the results in the measurements time region. In addition to the conventional NLS model [23]-[25], ΔV represents the voltage difference across the ferroelectric compared to the applied external voltage V_p due to the ferroelectric polarization, trapped charge, fixed charge, and work function differences (e.g. see Fig.11)

Before baking, the polarization switching time is well described by the NLS model (Fig. 8 (a)), similarly to what was reported in a MIM FE-HfO_2 capacitor [18]. After baking, the impact of imprint is clearly visible, but the trends here are still well described by the NLS model (Fig. 8(b)). The ΔV used in Eq. (2) was about +1.5 V larger than before baking, which is consistent with ΔV_c in Fig. (3)(a). Fig. 8(c) then shows P_{sw} after the application of 10 cycles of ±4 V pulses. Imprint is clearly recovered and all parameters except P_0 are the same as those before baking. The P_0 after recovery is the same as that after baking. This difference of the P_0 after baking seems to be independent of imprint because the P_0 cannot be recovered by additional pulses, in contrast to the imprint itself. The difference of the P0 might be mainly caused by the additional wake-up on the sample "before bake". (The switching pulses (high voltage to the lower voltage) were repeatedly applied on the same device for "before bake", which may cause additional wake-up and therefore a larger P0. Instead, for the samples of "after baking"

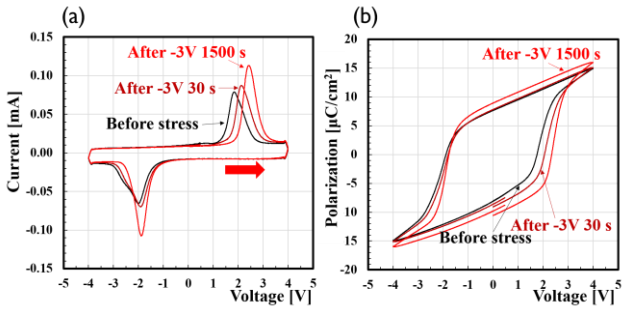

Fig. 10. (a) The I-V and (b) the corresponding P-V curves measured with a triangular pulse train with segment amplitudes of 0 V, +4 V, -4 V and 0 V for samples before bias stress, after bias stress for 30 sec and 1500 sec, respectively. The V_{c+} shifts toward positive values. The remanent polarization becomes larger due to the bias stress as well [20].

and "after recovery", the each switching pulse was applied on the different samples.) As a side note, the presented fitting parameters are not unique, however the trends of the results are the same with other parameters sets (e.g. assuming the full external voltage is applied to the FE: before baking: ΔV=0 V, α=0.7, μ=1.9 MV/cm, σ=1.3 MV/cm, after baking: ΔV=1.5 V, α=0.7, μ=2.6 MV/cm, σ=1.6 MV/cm).

The PDF, Eq. (3), and its cumulative density function (CDF) of samples have been simultaneously extracted (Fig. 9(a)). Moreover, switching time constants with the E_a corresponding to the CDF value of 0.9, τ_{90}, as a function of V_p are shown in Fig. 9(b). Thus, τ_{90} corresponds to the pulse duration required to switch 90% of the domains with each pulse amplitude. Interestingly, after baking, the PDF distribution becomes wider and shifts to larger values. Consequently, the difference of E_a corresponding to a CDF of 0.9 before and after bake becomes larger than that corresponding to a CDF of 0.5. As a result, the difference of pulse amplitude, ΔV_p >2.0 V, corresponding to the same τ_{90} becomes larger than the ΔV_c of ~1.5 V in Fig. (3)(a), which means that imprint is actually more severe for switching all of the domains than for switching half of the domains roughly corresponding to V_c. The root causes of the shift of the ΔV and the PDF widening are discussed in Section III-3.

On the other hand, after the application of recovery pulses, PDF and τ are the same as before recovery. The NLS model assumes that the switching time is dominated by the waiting time for the domain nucleation. Therefore, these results strongly indicate that *imprint is caused by an increased activation barrier of domain nucleation*, and furthermore, that this increased barrier can be recovered by additional pulses. In other words, these results support that imprint is caused by domain-seeds-pinning.

Possible origins of the increased activation barrier of domain nucleation have been argued to be electron charge trapping [8][9] or defect migration [19]. Then, in order to specify the origin, bias stress tests were carried out. After the application of wake-up pulses, negative bias stress of -3 V was applied for 30 s and 1470 s consecutively (Figs. 10(a) and (b)). The negative bias stress shifts the V_c in the positive direction (Fig. 10(a)). Moreover, ΔV_{c+} is larger than ΔV_{c-}, similar to the baking effect (cf. Fig. 1). The positive bias stress shows opposite results (not shown here). It is

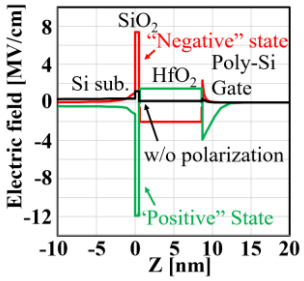

Fig. 11. Simulated electric field with gate voltage of 0V with polarization charge density of ±8 μC/cm² and 0 μC/cm² representing "positive" state, "negative" state and without ferroelectric polarization, assuming a relative permittivity of 30 for the HfO_2. [20].

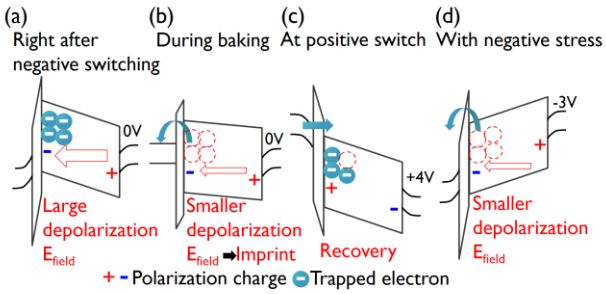

Fig. 12. Schematic of imprint model. (a) After negative switching following wake-up, (b) during baking, (c) at positive switching. (d) with negative stress.

difficult to explain these results by defect migration in FE-HfO_2 because the electric field in FE-HfO_2 induced by external negative bias must be opposite to that induced by spontaneous polarization of the "negative" state. Therefore, these results suggest that charge trapping is the probable cause of imprint.

3. CHARGE TRAPPING MODEL OF IMPRINT

Based on the results presented above, the detailed mechanisms of imprint are discussed in this section. We concluded in the last section that imprint is caused by charge trapping. To clarify the driving force of the charge trapping during baking, TCAD simulation was carried out (Global TCAD solutions software). The simulated structure was Poly-Si/HfO_2(8 nm) /SiO_2(0.5 nm)/Si, assuming a thin oxide IL between HfO_2 and Si substrate. The polarization effect was represented as fixed charges located at the Poly-Si/HfO_2 and the HfO_2/SiO_2 interfaces. As shown in Fig. 11, a high electric field is present in the IL of SiO_2 even at gate voltage of 0V due to the ferroelectric polarization. In addition, the polarization causes a depolarizing electric field in HfO_2 film.

Fig. 12 shows the schematic of the imprint model based on these results. After wake-up, and right after a negative sweep and back to 0V, polarization charges cause a high electric field in the IL and a large depolarization electric field in the FE-HfO_2 (Fig. 12(a)). During baking at the "negative" state, charge de-trapping of the electrons trapped in the FE-HfO_2 due to the high electric field in the IL reduces the depolarization field and can cause imprint (Fig. 12(b)). In other words, the charge de-trapping screens the internal electric field, which was represented by the difference of ΔV in the NLS model (2). In addition, the domain

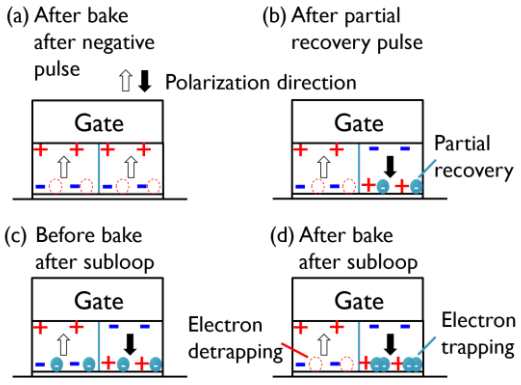

Fig. 13. Schematic with two remains of "partial recovery" and "sub-loop imprint". (a) after imprint subsequent to negative pulse (b) after partial recovery pulse (c) before bake after sub-loop, and (d) after bake after subloop.

to domain fluctuation in the number of trapped electrons may cause the wider distribution of the PDF as shown in Fig.9(a). If the volume of each domain is sufficiently small with respect to trapped electrons density, the impact of the fluctuation should be enhanced. A similar relationship between charge trapping and domain nucleation is described in [27].

Then, at subsequent positive switching, the electric field is drastically changed by switching polarization charge, leading to increased charge trapping (Fig. 12(c)). The charge trapping can result in a return to default trapped electron density, namely recovery from the imprint. In addition, the recovery from imprint leads to asymmetric V_c shifts (e.g. Figs. 1 and 3) as well. Once the domains are switched to the "positive" state, followed by a return to default trapped electron density, the electron occupation conditions at both V_{c-} of the 1st cycle and V_{c+} of the 2nd cycle become similar, consequently the $\triangle V_{c-}$ of the 1st cycle and the $\triangle V_{c+}$ of the 2nd cycle show the smaller V_c shifts than the $\triangle V_{c+}$ of the 1st cycle, leading to asymmetric V_c shifts, as shown in Fig. 3(b). These models can also describe the imprint corresponding to a "positive" state (cf. Fig. 6). During the baking at a "positive" state, electrons are trapped in the FE-HfO_2, reducing the depolarization electric field, and causing the imprint, i.e. V_c shifts to more negative voltages. In addition, the imprint can be recovered by charge de-trapping at negative switching.

Similarly, when the negative bias stress is applied, many trapped electrons are de-trapped as well as during baking (Fig. 12(d)). As a result, the negative stress shows similar results to the baking effect, as shown in Fig. 10(b). On the other hand, the "subloop imprint" (Fig. 6) shows that the imprint in each domain was not affected by the amplitude of a triangular pulse before baking. This is because the pulse duration was very short < 100μs, such that the charge trapping was dominated by the electric field (~ 10 MV/cm, see Fig. 11) caused by the polarization charge.

Figs. 13(a) and (b) show the schematics of the model of "partial recovery" from imprint shown in Fig. 4. After the baking subsequent to the application of the "negative" pulse, many electrons are de-trapped, leading to imprint (Fig. 13(a)). As shown in Fig. 11, the difference of the electric field is very large between each polarization direction. In other words, the polarization direction dominates the electric field and the electron occupation condition in each domain. Consequently, switching is indispensable for the recovery. Thus, after the application of the partial recovery pulse, some of the domains are switched followed by electron trapping, resulting in the "partial recovery" (Fig. 13(b)).

Our models can also describe the "sub-loop imprint" in Fig. 6, which clearly showed that imprint occurs independently in each domain. Figs. 13(c) and (d) show the schematics of the model of "sub-loop imprint". After the sub-loop test following wake-up, the FE-HfO_2 layer has both up-state domains and down-state domains simultaneously and the default trapped electron density in both domains as shown in Fig. 13(c). Then, after baking, electrons are de-trapped from the up-state domains, at the same time the electrons are additionally trapped in the down-state domains due to the large electric field in the IL in each domain individually (Fig. 13(d)). As a result, imprint occurs independently in each domain. Whereas, if the domain size were small and the domain wall were thin enough to be affected by the electric field from the neighboring domains, the imprint in each domain would depend on the states of the neighboring domains. Therefore, since according to our results, namely that imprint occurs independently in each domain, this also indicates the large size of domains, or the clustering of domains having the same states, or the presence of thick domain walls.

In Fig.12 and Fig. 13, the models described are based on charge trapping and de-trapping through the IL at the bottom interface. The models can be extended to charge trapping and de-trapping between the FE-HfO2 and the gate electrode when a non-ferroelectric layer is assumed at the top interface. In the latter case, the polarization charge at the top interface would cause a large electric field inducing charge trapping/de-trapping. In that case, the effect of imprint and its recovery would be the same as that for bottom interface. Moreover, the models can be applied to metal electrode FE capacitors too with the assumption a non-ferroelectric layer at the electrode interface.

IV. CONCLUSION

The results presented here strongly indicate that the imprint is caused by charge trapping or de-trapping in FE-HfO_2, which is consistent with the conclusions of recent publications [8][9]. Moreover, because the polarization direction dominates the trapped electron occupation condition in each domain, the domain switching leads to the charge trapping and de-trapping in the FE-HfO_2, resulting in imprint and its recovery. Furthermore, the recovery phenomena can explain the asymmetric shift between V_{c+} and V_{c-}. Based on the results obtained in this study, we conclude that, in order to ensure the reliability of the HfO_2 based FEFET memory, controlling the charge trapping and the resulting imprint are essential.

ACKNOWLEDGMENT

The authors acknowledge the contributions of S. Clima, U. Celano, A. Minj, V. Putcha, Z. Wu, Md Nur K. Alam, and S. V. Beek, in imec and K. Florent and A. Subirats now in Micron.

References

[1] K. Florent, M. Pesic, A. Subirats, K. Banerjee, S. Lavizzari,

A. Arreghini, L. Di Piazza, G. Potoms, F. Sebbai, S. R. C. McMitchell, M. Popovici, G. Groesneken and J. Van Houdt, "Vertical Ferroelectric HfO2 FET based on 3-D NAND Architecture: Towards Dense Low-Power Memory," in *2018 IEEE International Electron Devices Meeting (IEDM)*, San Francisco, CA, USA, 2018, pp. 2.5.1-2.5.4.

[2] H. Mulaosmanovic, E. T. Breyer, T. Mikolajick and S. Slesazeck, "Ferroelectric FETs with 20-nm-Thick HfO2 Layer for Large Memory Window and High Performance," *IEEE Trans. Electron Devices*, vol. 66, no. 9, pp. 3828-3833, 2019.

[3] K. Florent, S. Lavizzari, L. D. Piazza, M. Popovici, J. Duan, G. Groeseneken, J. V. Houdt, "Reliability Study of Ferroelectric Al:HfO2 Thin Films for DRAM and NAND Applications," *IEEE Trans. Electron Devices*, vol. 64, no 10, pp. 4091-4098, 2017.

[4] L. He and D. Vanderbilt, "First-principles study of oxygen-vacancy pinning of domain walls in PbTiO3," *Phys. Rev. B*, vol. 68, p. 134103, 2003.

[5] F. P. G. Fengler, M. Pessic, S. Starschich, T. Schneller, C. Künneth, U. Böttger, H. Mulaosmanovic, T. Schenk, M. H. Park, R. Nigon, P. Muralt, T. Mikolajick, U. Schroeder, "Domain Pinning: Comparison of Hafnia and PZT Based Ferroelectrics," *Adv. Electron. Mater.*, vol. 3, p. 1600505, 2017.

[6] D. Nagasawa and H. Nozawa," Imprint Model Based on Thermionic Electron Emission Under Local Fields in Ferroelectric Thin Films," *Jpn. J. Appl. Phys.*, vol. 38, pp. 5406-5410, 1999.

[7] A. Gruverman, B. J. Rodriguez, R. J. Nemanich and A. I. Kingon," Nanoscale observation of photoinduced domain pinning and investigation of imprint behavior in ferroelectric thin films," *Journal of Applied Physics*, vol. 92, pp. 2734-2739, 2002.

[8] F.P.G. Fengler, M. Hoffmann, S. Slesazeck, T. Mikolajick, and U. Schroeder," On the relationship between field cycling and imprint in ferroelectric $Hf_{0.5}Zr_{0.5}O_2$*," Journal of Applied Physics*, vol. 123, p. 204101, 2018.

[9] P. Buragohain, A. Erickson, P. Kariuki, T. Mittmann, C. Richter, P. D. Lomenzo, H. Lu, T. Schenk, T. Mikolajick, U. Schroeder, and A. Gruverman, "Fluid Imprint and Inertial Switching in Ferroelectric La:HfO_2 Capacitors," *ACS Appl. Mater. Interfaces*, vol. 11, pp. 35115-35121, 2019.

[10] Y. Zhou, H. K. Chan, C. H. Lam, and F. G. Shin, "Mechanisms of imprint effect on ferroelectric thin films," *Journal of Applied Physics*, vol. 98, p. 024111, 2005.

[11] C. K. Wong and F. G. Shin, "A possible mechanism of anomalous shift and asymmetric hysteresis behavior of ferroelectric thin films" *Appl. Phys. Lett.*, vol. 86, p.042901, 2005

[12] W. L. Warren, B. A. Tuttle, D. Dimos, G. E. Pike, H. N. Al-Shareef, R. Ramesh, and J. T. Evans, "Imprint in Ferroelectric Capacitors," *Jpn. J. Appl. Phys.*, vol. 35, pp. 1521-1524, 1996.

[13] K. Abe, N. Yanase, T. Yasumoto, and T. Kawakubo,"Nonswitching Layer Model for Voltage Shift Phenomena in Heteroepitaxial Barium Titanate Thin Films"*Jpn. J. Appl. Phys*., vol. 41, pp. 6065–6071 , 2002.

[14] H. Orihara, S. Hashimoto, and Y. Ishibashi, "A Theory of D-E Hysteresis Loop Based on the Avrami Model," *J. Phys. Soc. Jpn.*, 63, pp. 1031-1035, 1994.

[15] M. Avrami, "Kinetics of Phase Change. II Transformation-Time Relations for Random Distribution of Nuclei," *J. Chem. Phys.*, vol. 8, pp. 212-224, 1940.

[16] A. N. Kolmogorov and I. Akad, "On the Statistical Theory of Crystallization of Metals," Nauk SSSR, Ser. Mat., vol. 3, pp. 355-360, 1937

[17] A. K. Tagantsev, I. Stolichnov, N. Setter, J. S. Cross, and M. Tsukada, "Non-Kolmogorov-Avrami switching kinetics in ferroelectric thin films," *Phys. Rev.B*, vol. 66, p. 214109, 2002.

[18] N. Gong, X. Sun, H. Jiang, K. S. Chang-Liao, Q. Zia, and T. P. Ma, "Nucleation limited switching (NLS) model for HfO_2-based metal-ferroelectric-metal (MFM) capacitors: Switching kinetics and retention characteristics," *Appl. Phys. Lett.*, vol. 112, p. 262903, 2018.

[19] Y. Higashi, K. Florent, A. Subirats, B. Kaczer, L. Di Piazza, S. Clima, N. Ronchi, S. R. C. McMitchell, K. Banerjee, U. Celano, M. Suzuki, D. Linten and J. Van Houdt, "New Insights into the Imprint Effect in FE-HfO2 and its Recovery*,"* in *2019 IEEE International Reliability Physics Symposium (IRPS)*, Monterey, CA, USA, 2019, pp. 1-7, doi: 10.1109/IRPS.2019.8720553.

[20] Y. Higashi, N. Ronchi, B. Kaczer, K. Banerjee, S. R. C. McMitchell, B. J. O'Sullivan, S. Clima, A. Minj, U. Celano, L. Di Piazza, M. Suzuki, D. Linten and J. Van Houdt, "Impact of Charge trapping on Imprint and its Recovery in HfO2 based FeFET," in *2019 IEEE International Electron Devices Meeting (IEDM)*, San Francisco, CA, USA, 2019, pp. 15.6.1-15.6.4.

[21] T. Schenk, U. Schroeder, M. Pešić, M. Popovici, Y. V. Pershin, and T. Mikolajick, "Electric Field Cycling Behavior of Ferroelectric Hafnium Oxide", *ACS Applied Materials & Interfaces* 2014 6 (22), 19744-19751.

[22] M. Pešić, S. Slesazeck, T. Schenk, U. Schroeder, T. Mikolajick, "Impact of charge trapping on the ferroelectric switching behavior of doped HfO_2", Phys. Status Solidi A 213, No. 2, pp. 270-273, 2016.

[23] S. Zhukov, Y. A. Genenko, and H. V. Seggern, "Experimental and theoretical investigation on polarization reversal in unfatigued leadzirconate-titanate ceramic," *J. Appl. Phys.*, vol. 108. P. 014106, 2010.

[24] C. Alessandri, P. Pandey and A. C. Seabaugh, "Experimentally Validated, Predictive Monte Carlo Modeling of Ferroelectric Dynamics and Variability," in *2018 IEEE International Electron Devices Meeting (IEDM)*, San Francisco, CA, USA, 2018, pp. 16.2.1-16.2.4.

[25] Y. Xiang, M. Garcia Bardon, Md Nur K. Alam, M. Thesberg, B. Kaczer, P. Roussel, M. I. Popovice, L. -Å. Ragnarsson, B. Truijen, A. S. Verhulst, B. Parvais, N. Horiguchi, G. Groeseneken and J. Van Houdt, "Physical Insights on Steep Slope FEFETs including Nucleation-Propagation and Charge Trapping," in *2019 IEEE International Electron Devices Meeting (IEDM)*, San Francisco, CA, USA, 2019, pp. 21.6.1-21.6.4.

[26] W. J. Merz, "Switching Time in Ferroelectric BaTiO3 and Its Dependence on Crystal Thickness," *J. Appl. Phys.*, vol. 27, pp. 938-943, 1956.

[27] M. Pešić, A. Padovani, S. Slcsazeck, T. Mikolajick and L. Larcher, "Deconvoluting charge trapping and nucleation interplay in FeFETs: Kinetics and Reliability," in *2018 IEEE International Electron Devices Meeting (IEDM)*, San Francisco, CA, USA, 2018, pp. 25.1.1-25.1.4.